CONGRUENT AND INCONGRUENT DISSOLUTION OF LABRADORITE IN DILUTE, ACIDIC, SALT SOLUTIONS[1]

H. W. NESBITT, N. D. MACRAE, AND W. SHOTYK[2]
Dept. of Geology, Univ. of Western Ontario, London, Ontario, Canada N6A 5B7

ABSTRACT

Polished (001) cleavage faces of Nain Labradorite (An ≈ 56) were leached at 20°C (±2°) for 72 days in distilled water (pH ≈ 5.6), in HCl solution (pH ≈ 4.05) and in four other HCl solutions containing 1 mg/l or less of Na, K, Ca, Al(aq), and SiO_2(aq) (pH of all four solutions ≈ 4.05). Analysis of the cleavage faces by Secondary Ion Mass Spectrometry (SIMS) revealed no residual surface layer on faces leached by distilled water. By contrast, thick Si-rich residual layers (1500 Å) formed on surfaces leached by pure HCl solutions. Much thinner residual layers (700 Å) were observed on labradorite leached by HCl solutions containing 1 mg/l of Na, Ca, and K, whereas leached layers <75 Å thick formed on faces leached by solutions containing 1mg/l each of Na, K, Ca, Al(aq) and Si(aq); consequently *incongruent dissolution of feldspars* occurs in HCl solution, but *congruent dissolution of feldspars* occurs in mixed electrolyte solutions in which dissolved cations are more abundant than H_3O^+ (hydronium or proton). Of the cations studied, Al(aq) most affects formation of the leached layers, SiO_2(aq), however, does not noticeably affect thickness of the residual layer. Affinity of cations for surface functional groups affects the rate of formation of the leached layer (diffusion), and the rate of surface dissolution from the Si-rich surface layer, by controlling the concentration of H_3O^+ surface complexes on the surface of the leached layer. Diffusion through the leached layer apparently proceeds via lattice diffusion *and* line defects. A "competitive adsorption model" is proposed to explain the SIMS results and experimental leaching results of others. An important prediction of the model is that Si-rich residual layers generally do not form on feldspars of most soil and weathering profiles. If the residues form, they generally will be thin, with the thickness controlled by the composition of the soil solution.

INTRODUCTION

Berner and Holdren (1977) studied the surfaces of plagioclase and alkali feldspars and observed surface textural and morphological features that indicated that natural weathering of these minerals was controlled by reactions occurring at the feldspar-solution interface. Scanning electron microscopy (SEM) and X-ray photoelectron spectroscopy (XPS) studies of the surface and near-surface region indicated there was either no residual protective surface layer on the feldspars, or if present, the residual layer was at most a few 10s of angstroms thick. By contrast, recent leaching experiments and surface analytical studies of feldspars leached by HCl solutions under controlled conditions invariably demonstrate the existence of a Si-rich residual (leached) layer developed on the labradorite (Holdren and Speyer 1987, 1985; Chou and Wollast 1985, 1984; Muir et al. 1989, 1990; Casey et al. 1989, 1988; Hellman et al. 1989; Althaus and Tirtadinata 1989; Goossens et al. 1989; Westrich et al. 1989). These layers have undoubtedly formed in the experimental studies, but they have not been observed in naturally weathered feldspars (Nesbitt and Muir 1988; Keller 1978; Berner and Holdren 1979, 1977; Petrovic et al. 1976). This study addresses the obvious need to reconcile the experimental findings with the many studies of naturally weathered feldspars.

Stumm and co-workers (Stumm and Wollast 1990; Wieland et al. 1988) and Sposito (1984) argue that surface complex formation is a fundamental control on the rate at which minerals are weathered. The results of this study demonstrate that major cations (Na, K, Ca, Al) of soil waters are "complexed" by surface functional groups in preference to H_3O^+; thus the catalytic effect of the proton on feldspar dissolution is dramatically decreased as the concentrations of these solutes are increased.

Albitic and anorthitic exsolution lamellae exist in plagioclase of intermediate composition (Miura and Tomisaka 1978), such as the Nain labradorite of our experiments. The in-

---

[1] Manuscript received April 17, 1990; accepted July 11, 1990.

[2] Present address: Geologisches Institut, Universität Bern, CH-3012, Bern, Switzerland.

[Journal of Geology, 1991, vol. 99, p. 429–442]

0022-1376/91/9903-004$1.00

terfaces between the lamellae are a region of high strain and possibly structural mismatch, hence a region in which dislocations are concentrated. The diffusion rate of components may be greatly enhanced within these regions (Balluffi 1984). SIMS compositional depth profiles of the leached layers provide evidence that diffusion within line defects (such as the interfaces between the exsolution lamellae) occurs during formation of the experimentally produced Si-rich leached layers.

EXPERIMENTAL PROCEDURES

Sample Preparation and Treatment.—The average of five analyses by electron microprobe (using natural mineral standards on a Joel 8600 Superprobe) of the selected sample of Nain labradorite is $Ab_{43}An_{56}Or_1$. Standard deviations ranged for <1% for SiO_2 and Al_2O_3 to a maximum of 7.5% for K_2O.

Experimental procedures are similar (and the apparatus is identical) to those used by Muir et al. (1989, 1990). The labradorite sample was cleaved along the (001) face producing specimens measuring approximately 1cm diameter by 5 mm thick. The (001) perfect cleavage surfaces were then polished (6, 1, and ¼ μm diamond pastes) and cleaned with acetone followed by methanol. (Studies of both polished and unpolished surfaces indicate little effect of depth profiles obtained by SIMS; Ms in preparation.) Several slabs were immediately sealed in "zip-lock" polyethylene bags to be used as control samples; the remainder were placed on Teflon mesh inside six different 100 ml reaction vessels (polyethylene bottles).

All vessels were cleaned prior to use, following the same procedures as reported by Muir et al. (1989). Six different leaching solutions were prepared and stored in 1 L high-density polyethylene bottles (leachant vessels) on a shelf above the reaction vessels. Three solution vessels were used for the experiment. The *leachant vessel* was placed 50 cm above a sealed *reaction vessel* with the vessels connected by a 5 mm diameter polyethylene tube running from the base of the leachant vessel to the base of the reaction vessel. A third high-density polyethylene *collection vessel* was located 1 m below the reaction vessel. One end of a second 5 mm diameter polyethylene tube was connected to the reaction vessel near its top, and the other end was placed in the collection vessel. Solution flowed by gravity from the leachant vessel into the bottom of the sealed reaction vessel and out the top of the reaction vessel into the collection bottle. A stopcock on the tube connecting the leachant and reaction vessels was used to control the flow rate at approximately 250 ml per day. The flow rate was adopted to ensure that the pH of the reacted solution remained the same as the input, and to minimize concentration gradients or changes to the bulk solution composition around the reacting grains.

One leaching solution was distilled deionized water, prepared with a Millipore Milli-R/Q water purifier, and equilibrated with atmospheric CO_2 (pH = 5.6). For the other five experiments, a stock solution consisting of HCl diluted to 1.0×10^{-4} M/l (pH = 4.07 ± 0.05) was prepared. The first of the five leaching solutions was simply the stock HCl solution; the remaining four solutions were prepared by adding various amounts of reagent grade chloride salts of Na, K, Ca, and Al and aqueous silica (SiO_2 aq) to the HCl stock solution. The solution compositions are shown in table 1. Addition of the salts did not measurably affect pH of the stock HCl solution.

Following the run time of 72 days, the specimens were removed from the reaction vessels, gently rinsed with distilled water, and placed in "zip-lock" polyethylene bags. No additional treatment was required prior to analysis.

Analytical Techniques.—The leachants and leachates were analyzed by Atomic Absorption (AA) and Inductively Coupled Plasma Mass Spectrometry (ICP-MS) at the Soil Analysis Laboratory, Guelph University. The cations were detected but were too low to be quantitatively measured (all below 15 μ/l). Aqueous silica values were detected, but again the values were close to the levels of detectability (5–15 μgm/l). The low concentrations result from the high flow rates used to maintain a constant solution composition (in the reaction vessel) during dissolution. The lack of solution analyses is offset by the excellent results of Sjöberg (1989), who leached Nain labradorite in HCl solutions containing a variety of dissolved chloride salts. His results are discussed in detail subsequently, and interpreted in light of our studies.

Depth profiles of the leached and control labradorite samples were obtained using a Secondary Ion Mass Spectrometer (SIMS). The SIMS depth profiling technique is well established (Lovering 1975; Shimizu et al. 1978; Reed 1980; Steel et al. 1981), and its application to the study of feldspar leaching and weathering is documented (Nesbitt and Muir 1988; Muir et al. 1989). Instrumental settings and procedures are the same as reported by Nesbitt and Muir (1988) and Muir et al. (1989, 1990).

A CAMECA IMS 3f SIMS was used in specimen isolation (SI) mode (Metson et al. 1983, 1985; Nesbitt et al. 1986) to eliminate molecular ion interferences. The SI model requires no conductive coating or other treatment of the sample prior to analysis; thus no contaminants are introduced.

A primary ion beam of mass filtered $^{16}O^-$ at a net 15 to 16 kV and 110 nA was rastered over 250 × 250 μm area, with only positive secondary ions being analyzed. Crater edge effects were reduced using an aperture at the entrance to the spectrometer that accepted secondary ions from the central 50 μm of the rastered area. The analyzed area was sufficiently large to obscure surface compositional variations. Continual rastering of the beam eroded successive atomic layers, permitting analysis of the near-surface region as a function of depth. Sputtering rate for labradorite was close to 2 Å/s, albite, and oligoclase near 1.4 Å and 1.1 Å/s with a primary current of 110 nA (Muir et al. 1989, 1990). Accurate penetration rates were difficult to obtain because crater depths were inaccurate (Sloan Dektak profilometer). Surface irregularities remain after polishing, and irregular crater bottoms hamper accurate measurements. Also, leached surfaces may be sputtered at slightly different rates from fresh feldspar. A value of 2 Å/s per 100 nA primary current was used; real rates may differ by as much as 50%.

The isotopes ^{23}Na, ^{27}Al, ^{28}Si, ^{39}K, and ^{40}Ca were analyzed (fig. 1) using 1 s counting times. Each complete cycle, including time for magnet switching between masses, took 25 s. Approximately 40 cycles (1000 s total time) constituted each profile (fig. 1).

Data Treatment.—As apparent from figure 1, Al for example, is greatly depleted near the surface relative to Si, but secondary ion intensities are almost identical in the unleached interior of the grain. We illustrate compositional changes by calculating percent changes to the secondary ion intensity of each element (at each depth) relative to its intensity in the fresh labradorite, which is taken as the average of intensities of the five deepest analyses (considered to represent pristine, fresh labradorite). This is accomplished by two normalization calculations. The first requires the secondary ion intensity of each element "i" at depth "x," to be normalized to ^{28}Si (measured at same depth, $El_{i,x}/Si_{i,x}$), yielding $R_{i,x}$. $R_{i,x}$, then is normalized to the ratio of the same elements obtained for the pristine, fresh feldspar ($R_{i,p}$; average ratio for the deepest five analyses). The calculation is:

$$R_{i,s} = (El_{i,x}/Si_x)/(El_{i,p}/Si_p) \qquad (1)$$

where $R_{i,s}$ is the normalized ratio for element "i," at depth "x," for each sample "s." Normalization to ^{28}Si reduces the effects of primary current *fluctuations*. The following calculation reduces most systematic effects to secondary ion yields, including long-term drift, by normalizing $R_{i,s}$ (depth "x") to $R_{i,c}$, (same depth) of a control sample "c."

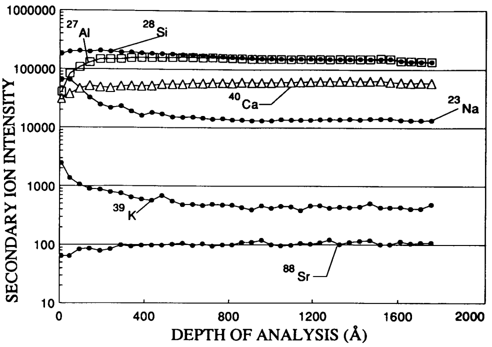

FIG. 1.—SIMS depth profiles of illustrating the secondary ion intensities of ^{23}Na, ^{27}Al, ^{28}Si, ^{39}K, and ^{40}Ca, plotted against depth. Zero depth represents the surface of the grain. Rate of penetration of the primary ion beam is 2 Å/s (see text). The profiles are of a (001) cleavage face of labradorite leached by HCl solution (table 1). Al, for example, is depleted near the surface relative to Si, but there is no depletion observed in unleached (control) samples or samples leached in distilled water (see Nesbitt and Muir 1988 for additional profiles).

$$\%\,\text{Change in } R_{i,s} = [(R_{i,s}/R_{i,c}) - 1] \times 100. \tag{2}$$

$R_{i,c}$ is identical to $R_{i,s}$, except it is the ratio for the unleached control sample, both being calculated for the same depth in each sample. The two-step procedure yields percentage changes in the leached samples relative to the fresh labradorite and relative to each depth "x" of the unleached control samples.

The procedure was applied to Al/Si (fig. 2) and Ca/Si (fig. 3). Profiles for Na and K were unusual in two respects: initial intensities were very high and decreased with depth, and the time to reach a steady state was very long (200 to 250 s; 400–500 Å depth) (fig. 1). These effects have been noted before (Havette 1985; Nesbitt and Muir 1988; Muir et al. 1989) and have been attributed to charge-induced migration of the elements within the surface layers. Because the effects tend to be particularly severe for Na, others (Muir et al. 1989) have ignored the Na data. Examination of Na/Si profiles indicates that time to reach steady state is influenced directly by Na content of the sample, and instrumental operating conditions. We conclude, therefore, that the Na/Si data can be compared only where (1) counts are normalized to a sample with similar Na content and (2) samples are analyzed during the same session, under the same operating conditions. Samples leached by pure distilled water and by HCl (HCl expt., table 1) were analysed during a different session than the other samples, hence are not included in the comparison (fig. 4*A*). Na/Si data from experiments 1, 2, and 4 are normalized to experiment 3 data (Fig. 4*A*). To test the reliability of the Na SIMS profiles, the Na/Si data for one SIMS Na profile (exp. 3) was normalized to a second Na profile of experiment 3 (Eq. 1) and the result plotted on figure 4*A*. Although fluctuations are evident, the two profiles are sensibly the same.

In spite of the charge-induced problem with K data (Nesbitt and Muir 1988), the effect is not as severe as for Na, thus data treatment was exactly as for Al and Ca with the exception that counting statistics were improved by combining the counts of two separate profiles (fig. 4*B*).

Reproducibility.—SIMS data were tested for reproducibility by collecting a minimum of two profiles of each leached sample. Figure 2 shows two Al/Si profiles for each of the six leaching experiments. Each profile (one plotted on figure 2*A*, the other on 2*B*) was obtained at a different location on the surface. Comparison of figure 2*A* and 2*B* provides the best evaluation of reproducibility because it includes all effects, including variability of surfaces and composition. The reproducibility is good for all profiles, but fluctuations increase with decreasing count rates, reflecting counting statistics.

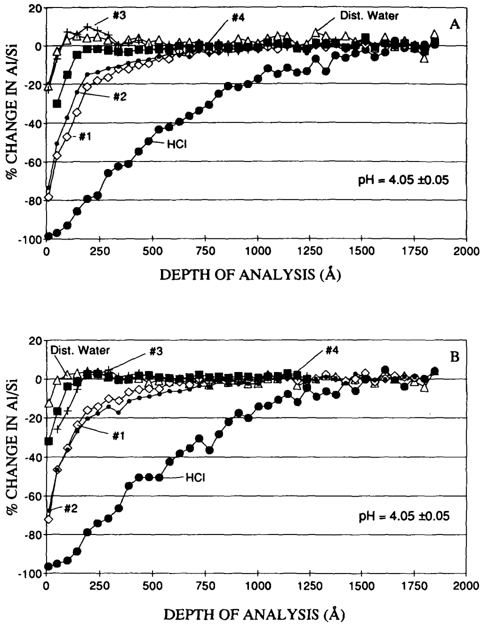

FIG. 2.—SIMS depth profiles $^{27}Al/^{28}Si$ illustrating the percentage change to the ratio of leached samples (relative to unleached labradorite) as a function of depth from the surface of the sample (see text and Muir et al. 1989 for normalization procedure). Leaching solution for the "Dist. Water" expt. is de-ionized, distilled water, and for the HCl experiment. 1.00×10^{-4} M/l HCl solution. The leaching solutions of exp. 1–4 are 1.00×10^{-4} M/l HCl stock solution to which 1.0 mg/l each of Na, K, and Ca have been added as well as different amounts of dissolved Al and Si (see table 1 for concentrations). The pH of all leaching solutions was 4.05 ± 0.05. The surface of the leached sample from each experiment was analyzed at least twice. The different profiles are shown on figure 1*A* and 1*B*. The profile was taken from widely separated spots on each sample; thus comparison of figure 1*A* and 1*B* provide a good guide to the reproducibility of the SIMS depth profiles.

RESULTS

Nain labradorite was leached by H_2O, HCl solutions, and solutions containing HCl and dissolved solids, NaCl, KCl, $CaCl_2$, $AlCl_3$,

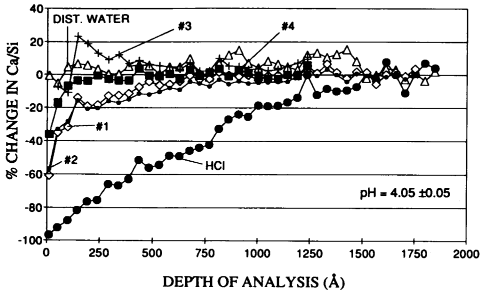

FIG. 3.—SIMS depth profiles of $^{40}Ca/^{28}Si$ illustrating the percentage change to the ratio of leached samples relative to unleached labradorite as a function of depth of analyses (see text and Muir et al. 1989 for normalization procedure). See table 1 for solution compositions for each experiment.

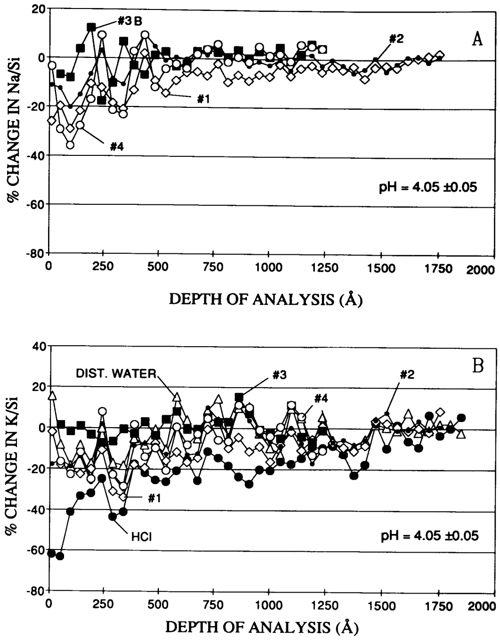

FIG. 4.—SIMS depth profiles of $^{23}Na/^{28}Si$ and $^{39}K/^{28}Si$ illustrating the percentage change to the ratio of leached samples (see text and Muir et al. 1989 for normalization procedure). See table 1 for solution compositions.

and $SiO_2(aq)$. The compositions of the different solutions are shown in table 1.

Treatment of labradorite samples with distilled water showed no effect to the labradorite surface after 72 days of leaching. All profiles, however, show fluctuations about the zero percent change value (figs. 2–4), and particularly nearest surface; the explanation for the variations is uncertain, but probably they are artifacts of the technique (Lau et al. 1985). Solutions before and after leaching, for all experiments, displayed no systematic or appreciable change in pH (table 1).

For the purpose of comparing and contrasting SIMS results, we show all Al/Si results in figure 2. Ca/Si results are grouped in figure 3. The Na/Si data have been treated differently to the rest in that data are normalized to the results of experiment #3 for the reasons explained in "Data Treatment." Na/Si profiles for near-surface zones of experiments 1, 2, and 4 show 15 to 30% depletion (fig. 4*A*); depletion is much less than for Ca/Si or Al/Si. K/Si data for experiments 1 and 2 show approximately 20% depletion in a surface leached zone but essentially no change (relative to the interior) for experiments 3 and 4. The K/Si and Na/Si profiles are sufficiently alike to conclude that both alkalis have responded similarly but differently from Ca, Al, or Si.

Si normalization (fig. 5) followed a slightly different procedure. Si secondary ion intensities were normalized to ^{28}Si of the pristine interiors of the grains (average of the deepest five analyses of each profile) and then normalized to the ^{28}Si of the control sample. There is no correction for fluctuations in primary beam intensity (see Eq. 1).

INTERPRETATION

Solutions were modeled using the SOLMINEQ program. Solution of experiment 4, which contains the most dissolved solids, requires a pH >4.4 to achieve saturation with respect to *crystalline* gibbsite, and still greater to be saturated in cryptocrystalline gibbsite or amorphous $Al(OH)_3$. The solutions are greatly undersaturated with respect Al-silicates.

Nature of Leached Layer.—All Element/Si ratios of labradorite samples leached by the stock HCl solution are low compared to the fresh mineral (i.e., Al, Ca, Na, and K are leached leaving a siliceous layer). These results confirm the findings of others (Casey et al. 1989, 1988; Muir et al. 1990, 1989; Chou and Wollast 1985; Holdren and Speyer 1985), who either detected siliceous leached layers, or to explain their experimental results, proposed that they formed. In the HCl experiment, profiles for Al/Si, Ca/Si, Na/Si, and K/Si change continuously from surface to un-

TABLE 1

DISSOLVED SOLIDS CONTENTS OF EXPERIMENTAL SOLUTIONS

	Exp. 1		Exp. 2		Exp. 3		Exp. 4	
Species	mg/l	Eq Fr[a]	mg/l	Eq Fr[a]	mg/l	Eq Fr[a]	mg/l	Eq Fr[q]
H(aq)[b]	. . .	.4566	. . .	.4543	. . .	.3030	. . .	.3030
Na(aq)	1.0	.1986	1.0	.1976	1.0	.1318	1.0	.1318
K(aq)	1.0	.1169	1.0	.1163	1.0	.0776	1.0	.0776
Ca(aq)	1.0	.2279	1.0	.2267	1.0	.1512	1.0	.1512
Al(aq)	.0	.0000	.01	.0050	1.0	.3364	1.0	.3364
Si(aq)	.0	.0000	1.0	.0000	1.0	.0000	.10	.0000
pH (Leachant)[c,e]		4.05		4.05		4.06		4.08
pH (Leachate)[d,e]		4.07		4.06		4.06		4.07

[a] Eq Fr = equivalent fraction of cationic charges.
[b] Concentration of hydronium ion calculated from pH measurements.
[c] pH of solution prior to reaction with labradorite (fig. 1).
[d] pH of solution after reaction with labradorite (fig. 1).
[e] Values quoted are averages; extreme over the 72 day period of the experiments are ±0.05 pH units.

leached interior; there is no evidence of "stepped" changes expected if crystalline, stoichiometric phases formed at the interface between solution and labradorite (Thompson 1957). Absence of stoichiometric relationships among the major elements implies that leached layers are predominantly noncrystalline, thus corroborating the results of Casey et al. (1988), who concluded that the siliceous leached layer was amorphous.

There are systematic changes to the Si profiles (fig. 5) in the leached zone. Data for the first 50 Å are difficult to interpret and not always reproducible, probably because of irregularities in surface topography and nonuniform initial surface charging (see Lau et al. 1985). The 100–500 Å depth intervals indicate ^{28}Si secondary ion yields similar to or slightly greater than that of fresh labradorite (especially for the HCl exp., exp. 1 and exp. 2, fig. 5). The increased yield may be due to the changing "matrix composition" in the leached zone, or it may result from the increased density of Si atoms; it is possible that the layer (virtually depleted of Al, Ca, and Na and structurally amorphous) may have collapsed, yielding a comparatively high Si density. Si-enrichment may result from low Si diffusivity through the leached layer; Shewmon (1968, p. 61) notes a low diffusivity for Si^{4+} in other crystalline phases.

Effects of Aqueous Ions on Leached Layers.—Solutions containing *only* HCl produce thick SiO_2-rich leached layers (fig. 2), whereas appreciably thinner residues form on labradorite leached by solutions containing dissolved Na, K, Ca, and Al. Although H_3O+ promotes surface dissolution of oxides and silicates (Wieland et al. 1988) including feldspars (Amrhein and Suarez 1988), the existence of the Si-rich layer is proof that surface dissolution proceeded less rapidly than formation of the leached layer. Our results demonstrate that the thickness of the leached layer is decreased by addition of dissolved salts to HCl solutions (fig. 2). There are two mechanisms by which this can be accomplished. Cations either inhibit formation of the leached layer (inhibit diffusion by "blocking" H_3O+ diffusive pathways), or they enhance surface dissolution rates to the extent that they proceed as rapidly as the formation of leached layers. Either effect decreases the thickness of (or eliminates) the residual layers.

Leached layers observed in these experiments indicate that Si remains as a residue, encasing fresh labradorite. As a result, the bulk of Si released to solution probably is derived from dissolution of the leached layer by detachment of silanol groups from the surface (Sposito 1984; Stumm and Wollast 1990). Sjöberg (1989 and our fig. 6) demonstrates clearly that addition of KCl (and NaCl) to solution decreases the release rate of Si *compared with its release rate in pure HCl solution* (fig. 6). Furthermore, the higher the concentration of K^+ in solution, the lower the release rate. Consequently, the thin leached layers observed for experiments 1–4 (com-

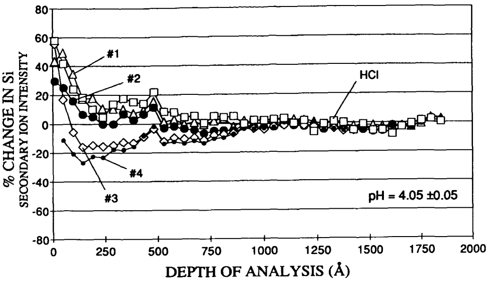

FIG. 5.—SIMS depth profiles of Si illustrating the percentage change in Si secondary ion intensities as a function of depth and relative to Si intensity of the unaltered interior of each grain. See table 1 for solution compositions.

pared with thickness of layer for the HCl exp) do not result from enhanced surface dissolution in KCl solution. The thin layers (experiments 1–4) must result from lower rates of formation of the leached layers, discussed below.

Dove and Crerar (1990) find that dissolved salts enhance the dissolution rate of quartz relative to its dissolution rate in distilled water. Dissolved salts may also enhance the rate of dissolution of feldspars compared with their dissolution rates in distilled water, but dissolved salts inhibit the dissolution rate of labradorite, *compared with its dissolution rate in pure HCl solution!*

Development and maintenance of the leached layer depends upon supply of protons from solution and rapid diffusion through the leached layer to the sites of feldspar leaching (Petit et al. 1987; Schott and Petit 1987; Casey et al. 1989). Three stages affect transportation of H_3O^+ through the leached layer (Boudart and Djega-Mariadassou 1984). First, H_3O^+ is adsorbed onto the surface (Sposito 1984; Stumm and Wollast 1990) of the leached solid; second, it must diffuse across the surface to a line defect (such as a twin boundary or dislocation); it finally must diffuse down the defect to the interior of the grain to sites of active feldspar leaching. Addition of salts to HCl leaching solutions results in competition among cations and H_3O^+ for surface sites or functional groups. By displacing H_3O^+ from the surface, the quantity of protons available for diffusion is diminished and the rate of formation of the layer is decreased.

The concentration of H_3O^+ in our experimental solutions is 1×10^{-4} M/l (table 1). In the HCl experiment, H_3O^+ is the only major, positively charged species available to react with surface functional groups; it is the only major positively charged species adsorbed. By contrast, H_3O^+ contributes 46% of positive charges to solution of experiment 1, 45% to the solution of experiment 2, and 30% to solutions of experiments 3 and 4; thus in these mixed electrolyte solutions there is competition amongst H_3O^+ and the other cations for surface sites and surface functional groups. The probability that a species is adsorbed (forms a surface complex) is determined by its concentration (table 1) and by the strength (association constant) of the surface complex. Dugger et al. (1964) provide free energy data for reaction between cations (Me^{n+}) and Si-O^- surface functional groups of amorphous silica:

$$\underset{\text{cation}}{\mathrm{Me}^{n+}} + \underset{\substack{\text{surface}\\\text{group}}}{n\mathrm{Si\text{-}O}^-} = \underset{\substack{\text{surface}\\\text{complex}}}{\mathrm{Me(Si\text{-}O)}_n} \qquad (3)$$

The data are directly applicable to the surfaces of the leached layers in that they are amorphous and Si-rich. Li^+ forms a weak surface complex compared with H_3O^+ (Dugger et al. 1964); thus it is unlikely to displace H_3O^+ from silanol surface groups. By contrast, surface complexes of the other alkalis, the alkaline earths, and the more highly charged cations are stronger than the H_3O^+ complex, as indicated by their association constants. These cations are, as a result, likely to displace H_3O^+ from surfaces, decrease the concentration of protons on the surfaces, and inhibit or prevent formation of Si-rich leached layers.

The experiments of Sjöberg (1989) confirm these predictions. He leached Nain labradorite in 0.01 M HCl for 1700 hr (fig. 6). Na, Ca, and Al were preferentially leached over Si in both solution compositions (fig. 6); thus Si-rich residual layers formed on labradorite, just as observed in our experiments. Comparison with our results (labradorite leached in solutions of pH = 4.0 for 1728 hr) indicates that the leached layers produced by Sjöberg (1989) were 1000s of angstroms thick. Westrich et al. (1989) observed leached layers several 100s of angstroms thick on labradorite

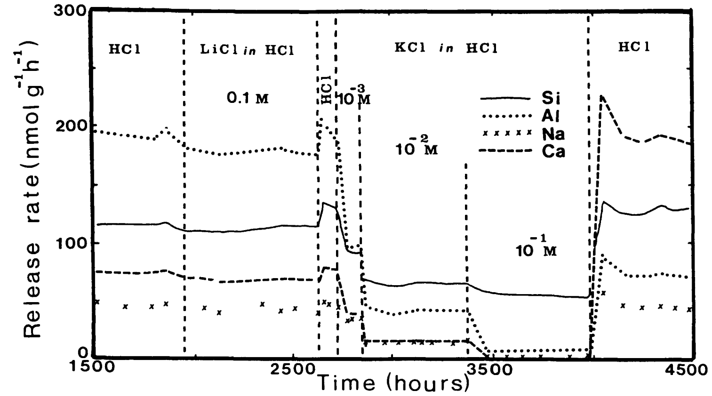

FIG. 6.—Experimental results of Sjöberg (1989) showing the release rates of Na, Al, Si, and Ca from Nain Labradorite during dissolution in HCl solutions (pH = 2.0) containing LiCl and KCl at 25°C (diagram modified after Sjöberg 1989). Release rates of all elements are decreased with addition of KCl (and NaCl) to HCl solutions.

leached for only 400 hr by 0.01 HCl solutions. Addition of LiCl to HCl solution has little effect on release rates of Na, Al, Si, or Ca (fig. 6). We conclude that even where Li^+ and H_3O^+ are present in solution at equal concentrations (fig. 6), Li does not interfere with the actions of the proton, including proton fixation on the surface of the leached layer and diffusion through the leached layer.

Addition of 0.001 M KCl to solution (fig. 6, 2600 hr) decreases the release rates of all major constituents. Also, the greater the amount of KCl added, the lower the release rates of the elements (fig. 6). The bulk of Na, Ca, and Al is derived from breakdown of labradorite in the interior of the grain (the thick Si-rich residual layer is already leached of these elements, figs. 2 and 3); consequently the diminished release rates of Na, Ca, and Al reflect decreased rates of labradorite breakdown. Breakdown of the feldspar, however, is determined by the rate of supply of protons; thus supply of protons must be inhibited by addition of KCl. This can be accomplished where K^+ displaces H^+ from the surface (as predicted from the data of Dugger et al. 1964), decreasing the H^+ chemical potential at the surface, diminishing the H^+ gradient across the leached layer, and necessarily decreasing the flux of H^+ to the interior of the grain. Sjöberg (1989) notes that addition of NaCl has the same effect. The data of Dugger et al. (1964) indicates that Al surface complexes are very strong. It should be very effective at displacing the H^+ from the surface, and apparently it is because addition of only 1 mg/l of Al(aq) to HCl solution (pH = 4.0) effectively eliminated the leached layer in experiment 4.

Competition between H_3O^+ and cations for surface sites determines the rate of formation of the leached layer. If so, uncharged and negatively charged species have little effect on the rate of formation or thickness of the leached layers. Our results (experiments 1, 2, 3 and 4) demonstrate that SiO_2(aq) has little affect on the thickness (hence rate of production) of the leached layer (fig. 2). Aqueous silica is neutrally charged in these acidic solutions, and not in a form to act as a competitor for the same surface functional groups as H_3O^+. Anions similarly should not compete for the same surface sites as the proton; hence Cl^- should not affect feldspar dissolution rates. Experimental results of Sjöberg (1989) demonstrate that Cl^- has no measurable effect on the rate of production or thickness of leached layers, otherwise addition of LiCl would have affected leach rates (fig. 6).

We conclude that addition of K^+, Na, Ca, and Al change the relative rates of reaction in favor of surface dissolution by decreasing dramatically the rate at which H^+ diffuses into the leached layer (to attack fresh feldspar). Decreased fluxes of H^+ are achieved wherever cations compete successfully with the proton for surface functional groups (adsorption). Results of Sjöberg (1989), who monitored solution compositions, our SIMS data, and the data of Dugger et al (1964) are all in accord, and the combined results provide the insight needed to predict the effects of individual cations on leaching characteristics of feldspars.

Comparison of Profiles in Leached Layers.—A striking feature of the SIMS results is the similarity between Ca/Si and Al/Si depth profiles (fig. 3). In fact, Ca and Al are leached from the solid in the proportion present in the mineral. The observation is confirmed by Sjöberg (1989), who shows that Ca/Si of labradorite and leachates are identical within reproducibility of the data. Ca(aq)/Al(aq) is 0.39 (± 0.05, molar ratio) in HCl solutions (fig. 6), which is close to the molar ratio of Ca/Al in Nain labradorite (0.36 ± 0.04, electron microprobe). Sjöberg (1989) demonstrates that the relationship holds for leachants containing HCl + KCl.

Na/Si and K/Si profiles (fig. 4) are similar but much different from the Ca/Si and Al/Si depth profiles (figs. 2, 3). The alkalis are necessarily leached at a rate different from Ca or Al, and different from alkali/Ca and alkali/Al values of fresh labradorite. The observation is again confirmed by the leaching study of Sjöberg (1989), where it is shown that HCl and HCl + KCl leachants contain low Na/Ca (and Na/Al) ratios relative to these ratios in fresh labradorite.

Although Na and K behave differently from Ca and Al during leaching, our experiments provide no explanation for the observation. Behavior of these elements, however, may be related to structural and compositional properties of the Nain labradorite. Crystallographic studies (Miura and Tomisaka 1978; McConnell 1974) show that Nain labradorite, and intermediate plagioclases generally, consist of albite-rich and anorthite-rich exsolution lamellae, approximately 2000 Å thick, giving rise to the observed schiller effects. Muir et al. (1990) show that anorthitic plagioclase dissolves more rapidly than albitic plagioclase in HCl solution. This observation, applied to albitic and anorthitic exsolution lamellae of Nain labradorite, would explain the differences in leach rate of the alkalis, Ca, and Al. The release of Na and K is controlled by relatively slow leaching of the albitic lamellae, whereas the anorthitic lamella dissolve more rapidly and control release of Ca and Al to solution. The exsolution lamellae of Nain plagioclase also have important implications for the mechanism of leaching.

Compositional Gradients and Diffusion.—Compositional gradients within the leached layers are related to the depth profiles (figs. 2–5) according to:

$$M(i,s)/M(Si,s) = [\%\ \text{CHANGE in R}] \times M(i,c)/M(Si,c) \tag{4}$$

where [% CHANGE in R] is defined by Eq. 2, M(i,s) is the molar concentration of element "i" at depth "x" in the leached sample, and M(i,c) is the molar concentration of "i" in the control sample at depth "x." There is little change to the secondary ion intensity of Si in the leached layers (fig. 5, except within 100 Å of the surface); hence M(Si,s) is approximately equal to M(Si,c) and Eq. 4 reduces to:

$$M(i,s) \approx [\%\ \text{CHANGE in R}] \times M(i,c)$$

The difference between [% CHANGE in R] and the concentration of element "i" in the leached sample [M(i,s)] is a constant, M(i,c). The depth profiles of figure 2–4 reflect, therefore, compositional gradients for each element "i." These figures are converted to compositional gradients by multiplying the ordinate by the scale factor M(i,c). Actual compositional gradients are not shown because the profiles of figures 2–4 mimic the compositional gradients. Profiles are referred to as compositional gradients in the following interpretation.

Generation and maintenance of the Si-rich leached layer results from diffusion of H^+ into, and Na, K, Ca and Al (in preference to Si) out of the leached layer. Provided just one standard state chemical potential is applied to each element within the leached layer, the compositional (concentration) gradient reflects directly the chemical potential gradient. These gradients change continuously with respect to time, until the steady state is achieved. There are now many studies that demonstrate the existence of compositional gradients within leached layers (Hellman et al. 1990; Muir et al. 1988, 1989; Casey et al. 1988), and the properties of these gradients may provide insight into the diffusion process.

Diffusion proceeds both through the bulk sample (bulk, volume, or lattice diffusion) and along line and planar defects such as twin boundaries and dislocations (short-circuit or high-diffusivity paths; Turnbull, 1951; Gibbs and Harris 1969; Peterson 1980; Balluffi 1984; Le Claire and Rabinovitch 1984). The interfaces between the albitic and anorthitic exsolution lamellae of Nain labradorite are zones of high strain and possibly of lattice misfit and undoubtedly contain a high concentration of lattice defects, particularly dislocations (Balluffi 1984). These zones and twin boundaries are the likely locations of line defects in the feldspar (Holdren and Speyer 1985, 1987).

Lattice and coupled lattice/dislocation diffusion theory (Shewmon 1963; 1969; Le Claire and Rabinovitch 1984) are used to evaluate which diffusional pathways contribute to the creation of the leached layers. Leached layers 1500 Å thick were produced in the HCl experiments, but the thickness of labradorite slabs used in the experiments is 0.5 cm; thus the slab is infinitely thick for the purpose of modeling. The leachant flows through the reaction vessel at a very rapid rate compared with the rate of leaching; hence the solution contacting the solid is considered to be of constant composition during the entire experiment. These constraints and a constant value for the diffusion coefficient yield the following equation for lattice diffusion (Shewmon 1969, Eqs., 2-16, 2-20):

$$M_x(i,t) = M_s(i) - [M_s(i) - M_o(i)\mathrm{erf}[\times/2D_i(t)] \qquad (5)$$

where $M_x(i,t)$ is the concentration of element "i" at distance "x" from the solution-solid interface at time "t." $M_s(i)$ is the concentration of "i" at the surface of the solid, and $M_o(i)$ is the concentration of "i" in the fresh, unleached solid. D_i is the diffusion coefficient of "i" in the leached layer and "erf" is the error function. The initial conditions are:

at t = 0: $M_o(Al)$ = 1.55 mole/mole of plagioclase
$M_s(Al)$ = 0.00 mole/mole of solid at the interface (HCl exp.)
= 0.45 mole/mole of solid at the interface (exp. 1, 2)
= 0.30 mole/mole of solid at the interface (exp. 3, 4)

They are considered to remain constant for the entire experiment ($t > 0$). The diffusion coefficients are trial-and-error values chosen to fit the first few hundreds of angstroms of the SIMS profiles (300 Å for fig. 7*A*, 200 Å for fig. 7*B*, and 100 Å for fig. 7*C*).

In the HCl experiment, $D_{Al} = 4.6 \times 10^{-18}$ cm^2/s and the appropriate initial conditions were used to calculate the compositional gradient. The percentage change to Al/Si then was calculated (no gradient in Si was assumed), and the result plotted on figure 7*A* as the solid curve. Four separate SIMS profiles of leached labradorite from the HCl experiment are included, D_{Al} was set to 2.3×10^{-19} cm^2/s, and the appropriate initial conditions were adopted to calculate the compositional gradients, and Al/Si ratios for experiments 1 and 2 (fig. 7*B*, dashed curve). Finally, a D_{Al} value of 4.6×10^{-20} cm^2/s and requisite initial conditions were used to calculate the compositional and Al/Si profiles for experiments 3 and 4 (fig. 7*C*, dashed curve).

The curve of figure 7*A* conforms to the trends of the SIMS data throughout the leached layer. The compositional gradient and SIMS Al/Si profiles for the HCl experiment are most simply explained to be the result of bulk (lattice) diffusion. By contrast, the calculated Al/Si trend of figure 7*b* duplicates only the initial trend of the SIMS data but does not (and cannot) reproduce the data in the region between 200 Å and 700 Å depth (the "tail" of the profile). The slope of the tail is much shallower than predicted for lattice diffusion, and the tail extends much deeper into the mineral than predicted from lattice diffusion theory. These are characteristics of rapid diffusion within twin boundaries and dislocations (Le Claire and Rabinovitch 1984). Diffusion along line defects apparently occurs during formation of leached layers of experiments 1 and 2. The SIMS data of figure 7*C* and the calculated and observed Al/Si profiles for experiments 3 and 4 are in accord. The leached layers are so thin, however, that the data may be more affected and better explained by very near-surface reactions, such

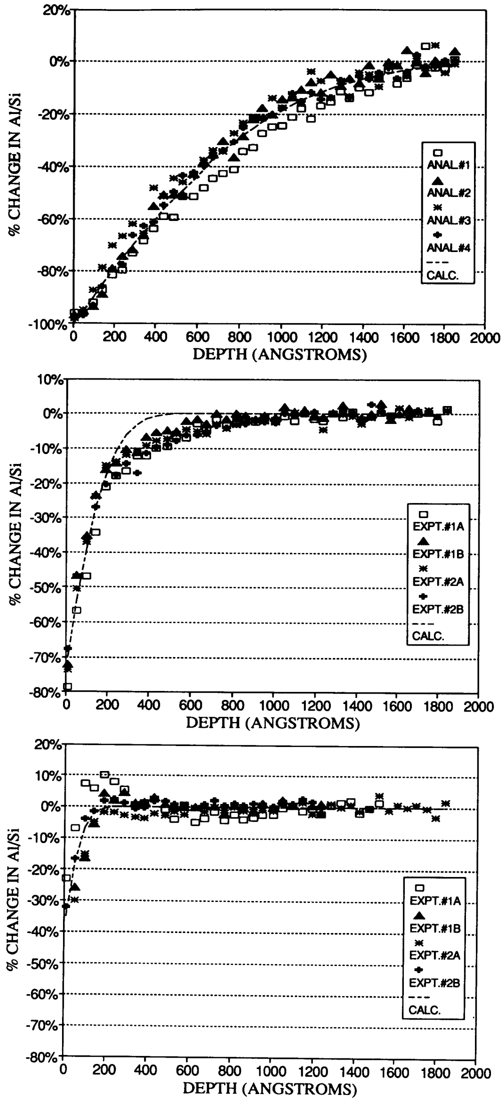

FIG. 7.—SIMS depths profiles for Al/Si compared with profiles calculated assuming lattice diffusion (Eq. 5). Figure 7*A* illustrates four separate SIMS depth profiles of the 001 cleavage face of labradorite from the HCl experiment. 7*B* illustrates two SIMS profiles of the 001 cleavage face of each labradorite sample leached in exps. 1 and 2 (table 1). The dashed curve is calculated from Eq. 8 to fit the SIMS data of the first 200 Å. Figure 7*C* illustrates two SIMS profiles of the 001 cleavage face of each labradorite sample leached in exps. 3 and 4 (table 1). Lattice diffusion theory does not explain the compositional profiles observed in exps. 1 and 2.

as cation exchange and selective dissolution of elements.

The apparent absence of diffusion "tails" from the leached layers of the HCl, #3 and #4 experiments is explained by Le Claire and Rabinovitch (1984, p. 280–283). Their treatment suggests that the HCl-generated profile and the profiles of experiments 3 and 4 may be the type referred to as the "linear domain," whereas the profiles of experiments 1 and 2 are composite "gaussian/linear." Comparison of the calculated and experimental results indicates that diffusion along line defects (dislocations and twin boundaries) contributes to generation of leached layers. Additional discussion requires extension of their mathematical treatment to include the conditions specific to these experiments.

LEACHING OF FELDSPARS IN SOILS

Berner and Holdren (1977, 1979) and Holdren and Berner (1979) argue that the weathering of feldspars in soils is controlled by chemical reactions at the feldspar-solution interface. SEM and XPS studies (Berner and Holdren 1977; Petrovic et al. 1976) indicate that leached layers no more than a few 10s of angstroms thick exist on naturally weathered feldspars. No Si-rich layers 100s to 1000s of angstroms thick (such as produced by HCl solutions) were detected. The SIMS data resolve the apparently conflicting experimental and natural weathering results. Most common cations, even at very low concentrations, reduce the leached layer to 50 Å or less, as found in experiments 3 and 4 of this study.

Effective elimination of the leached layer requires that the concentration of cations be approximately equal to or greater than the concentration of H_3O^+ in solution. The pH of soil solutions is typically 4 to 5; the requisite concentration of $Ca^{2+}(aq)$, for example, required to eliminate leached layers would be 1×10^{-4} to 1×10^{-5} M/l (0.4 to 4 mg/l) (depends upon the association constant of the surface complex). Generally, leached layers will be absent from feldspars where the sum of dissolved Na, K, Ca, and Mg (common cations) are 1 to 4 mg/l. The range is comparable to, or lower than, most soil solutions (Manley et al. 1987); consequently extensive Si-rich leached layers are not likely to be found on feldspar grains. The SIMS study and the "competitive adsorption" hypothesis derived from the results confirm the findings, arguments, and conclusions of Berner and Holdren and also explain the development of Si-rich leached layers in experimental HCl solutions.

CONCLUSIONS

Labradorite cleavage surfaces (001) leached by distilled water showed no detectable (<50 Å) alteration layers. A SiO_2-rich residual layer 1500 Å thick was formed by leaching with HCl solution (pH $\approx$ 4.0–4.1), confirming results of others. Leaching by HCl solution (pH $\approx$ 4.1) containing 1.0 mg/l of Na, K, and Ca (no Al or Si) produced a 700 Å thick SiO_2-rich residual layer. Solution (pH $\approx$ 4.1) containing 1.0 mg/l each of Na, K, Ca, SiO_2(aq) and 0.01 mg/l Al(aq) produced a leached layer, again 700 Å thick, and indistinguishable from the previous experiment. By contrast, an acidic solution (pH $\approx$ 4.1) containing 1.0 mg/l of Na, K, Ca, Al(aq) and SiO_2(aq) produced a SiO_2-rich residual layer 50 Å thick. Of the dissolved solutes, Al(aq) has the greatest effect on the composition and thickness of the residual layers; Si(aq) has little effect.

Siliceous, probably amorphous, leached-layers develop on labradorite during attack by HCl solutions (pH $\approx$ 4.0). The thickness of the leached layer is controlled by the relative amounts of H_3O^+ and cations in solution, Cations which compete successfully with H_3O^+ for surface functional groups (adsorption sites) inhibit the adsorption of hydronium ion, and the supply of H_3O^+ to the interior of grains where active feldspar leaching occurs. Thicknesses of leached layers are substantially reduced where the sum of the concentrations of common cations is approximately equal to the concentration of hydronium ion. The leached layers are effectively eliminated where the concentration of these cations are greater than that of H_3O^+.

The leached layer is produced and maintained by diffusion of hydronium ions from the solution-solid interface through the leached layer to sites where labradorite is actively altered. Transport through the leached layer occurs by lattice diffusion and by diffusion along line defects generally, dislocations, and twin boundaries.

The "competitive adsorption" hypothesis is proposed to explain our SIMS results. An important prediction of the hypothesis is that siliceous leached layers do not form on feldspars of soils because the concentrations of Na, K, Ca, Mg and Al in soil solutions generally are greater than the concentration of H_3O^+. Our SIMS results and the hypothesis confirm the findings, arguments, and conclusions of Berner and Holdren (1977); feldspars dissolve congruently in acidic soil solutions. Only where hydronium ion is the most abundant cationic species in leachants will Si-rich leached layers form on feldspars. Such solutions are restricted largely to the laboratory, although increased acid deposition may result in solutions in which H_3O^+ is the dominant cationic species.

ACKNOWLEDGMENTS.—I. Muir provided, and J. Forth polished the mineral specimens. Kim Law and L. Deakin prepared the solutions and monitored the leaching experiments. We are thankful for their time and effort. SIMS analyses were performed at the Surface Science Western Laboratories (operated by NDM). We thank Rich Holdren for his encouragement, for reading an early version of the Ms, and for offering valuable advice and insight into the leaching of feldspars. We also thank the reviewers for their critical evaluation of the Ms. The research was supported by grants from the Ontario Ministry of the Environment, including an eight month research associate position for one of us (WS), and from the National Sciences and Engineering Research Council of Canada.

REFERENCES CITED

ALTHAUS, E., and TIRTADINATA, E., 1989, Dissolution of feldspar: the first step, *in* MILES D. L., ed., Water-Rock Interaction: Rotterdam, Balkema, p. 15–17.

AMRHEIN, C., and SUAREZ, D. L., 1988, The use of a surface complexation model to describe the kinetics of ligand-promoted dissolution of anorthite: Geochim. Cosmochim. Acta, v. 52, p. 2785–2793.

BALLUFFI, R. W., 1984, Twin boundary diffusion mechanisms in metals, *in* MURCH, G. E., and NOWICK, A. S., eds., Diffusion in crystalline solids: Orlando, Academic Press, p. 319–377.

BERNER, R. A., and HOLDREN, G. R., 1977, Mechanisms of feldspar weathering. Some observational evidence: Geology, v. 5, p. 369–372.

———, and ———, 1979, Mechanisms of feldspar weathering—II. Observations of feldspars from soils: Geochim. Cosmochim, Acta, v. 43, p. 1173–1186.

Boudart, M., and Djega-Mariadassou, G., 1984, Kinetics of Heterogeneous Catalytic Reactions: Princeton, NJ, Princeton Univ. Press, 222 p.

Casey, W. H.; Westrich, H. R.; and Arnold, G. W., 1988, Surface chemistry of labradorite feldspar reacted with aqueous solutions at pH = 2, 3, and 12: Geochim. Cosmochim. Acta, v. 52, p. 2795–2807.

———; ———; ———; and Banfield, J. F., 1989, The surface chemistry of dissolving labradorite feldspar: Geochim. Cosmochim. Acta, v. 53, p. 821–832.

Chou, L., and Wollast, R., 1984, Study of weathering of albite at room temperature and pressure with a fluidized bed reactor: Geochim. Cosmochim. Acta, v. 48, p. 2205–2217.

———, and ———, 1985, Steady-state kinetics and dissolution mechanisms of albite: Am. Jour. Sci., v. 285, p. 963–993.

Dove, P. M., and Crerar, D. A., 1990, Kinetics of quartz dissolution in electrolyte solutions using a hydrothermal mixed flow reactor: Geochim. Cosmochim. Acta, v. 54, p. 955–969.

Drever, J. I., 1988, The Geochemistry of Natural Waters: Englewood Cliffs, NJ, Prentice Hall, 437 p.

Dugger, D. L.; Stanton, J. H.; Irby, B. N.; McConnell, B. I.; Cummings, W. W.; and Maatman, R. W., 1964, The exchange of 20 metal ions with the weakly acidic silanol group of silica gel: Jour. Phys. Chem., v. 68, p. 757–760.

Gibbs, G. B., and Harris, J. E., 1969, Interfaces Conference: Melbourne, Aust. Inst. Metals and Butterworths, 364 p.

Goossens, D. A.; Philippaerts, J. G.; Gijbels, R.; Pijpers, A. P.; Van Tendeloo, S.; and Althaus, E., 1989, A SIMS, XPS, SEM, TEM, and FTIR study of feldspar surfaces after reacting with acid solutions, *in* Miles, D. L., ed., Water-Rock Interactions: Rotterdam, Balkema, p. 271–274.

Havette, A., 1985, Mineralogical application of the ion microscope: Scanning Electron Microscopy, v. 2, p. 585–594.

Hellman, R.; Eggleston, G. M.; Hochella, M. F.; and Crerar, D., 1990. The formation of leached layers on albite surfaces during dissolution under hydrothermal conditions. Geochim. Cosmochim. Acta, v. 54, p. 1267–1281.

Holdren, G. R., and Berner, R. A., 1979, Mechanisms of feldspar weathering: I. Experimental Studies: Geochim. Cosmochim. Acta, v. 43, p. 1161–1171.

———, and Speyer, P. M., 1985, pH dependent changes in the rates and stoichiometry of dissolution of an alkali feldspar at room temperature: Am. Jour. Sci., v. 285, p. 994–1026.

———, and ———, 1987, Reaction rate-surface area relationships during the early stages of weathering. II. Data on eight additional feldspars: Geochim. Cosmochim. Acta, v. 51, p. 2311–2318.

Keller, W. D., 1978, Kaolinization of feldspar as displayed in scanning electron micrographs: Geology, v. 6, p. 184–188.

Le Claire, A. D., and Rabinovitch, A., 1984, The mathematical analysis of diffusion in dislocations, *in* Murch, G. E., and Nowick, A. S., eds., Diffusion in Crystalline Solids: Orlando, Academic Press, Inc., p. 257–318.

Lovering, J. F., 1975, Applications of SIMS microanalysis techniques to trace element and isotopic studies in geochemistry and cosmochemistry: U.S. Natl. Bur. Stand. Spec. Pub., v. 427, p. 135–178.

Manley, E. P.; Chesworth, W.; and Evans, L. J., 1987, The solution chemistry of podzolic soils from the eastern Canadian shield, a thermodynamic interpretation of the mineral phases controlling soluble Al^{3+} and H_4SiO_4: Jour. Soil Science, v. 38, p. 39–51.

McConnell, J. D. C., 1974, Electron-optical study of the fine structure of a schiller labradorite, *in* McKenzie, W. S., and Zussman, J., eds., The Feldspars: Manchester, Manchester Univ. Press, (NATO Adv. Studies Inst.), p. 478–490.

Metson, J. B.; Bancroft, G. M.; McIntyre, N. S.; and Chauvin, W. J., 1983, Suppression of molecular ions in the secondary ion mass spectra of minerals: Surface and Interface Analysis, v. 5, p. 181–185.

———; ———; and Nesbitt, H. W., 1985, Analysis of minerals using specimen isolated secondary ion mass spectrometry: Scanning Electron Microscopy, v. 2, p. 595–603.

Miura, Y., and Tomisaka, T., 1978, Ion microprobe mass analysis of exsolution lamellae in labradorite feldspar: Am. Mineral., v. 63, p. 584–590.

Muir, I. J.; Bancroft, G. M.; and Nesbitt, H. W., 1988, Characteristics of altered labradorite surfaces by SIMS and XPS: Geochim. Cosmochim. Acta, v. 53, p. 1235–1241.

———; ———; Shotyk, W.; and Nesbitt, H. W., 1990, A SIMS and XPS study of dissolving plagioclase: GCA, in press.

Nesbitt, H. W.; Metson, J., B.; and Bancroft, G. M., 1986, Quantitative major- and trace-element whole-rock analyses by secondary-ion mass spectrometry using the specimen isolation technique: Chem. Geol., v. 55, p. 139–160.

———, and Muir, I, J., 1988, SIMS depth profiles of weathered plagioclase and processes affecting dissolved Al and Si in some acidic soil solutions: Nature, v. 334, p. 336–338.

Peterson, N. L., 1980, Twin Boundary Structure and Kinetics: Metals Park, Ohio, Am. Soc. Metals. 209 p.

Petit, J. C.; Mea, G. D.; Dran, J. C.; Schott, J. S.; and Berner, R. A., 1987, Mechanism of diopside dissolution from hydrogen depth profiling: Science, v. 325, p. 705–707.

Petrovic, R.; Berner, R. A.; and Goldhaber, M. B., 1976, Rate control in dissolution of alkali feldsparss—I. Study of residual feldspar grains by X-ray photoelectron spectroscopy: Geochim. Cosmochim. Acta, v. 40, p. 537–548.

REED, S. J. B., 1980, Trace element analysis with the ion probe: Scanning, v. 3, p. 119–127.

SCHOTT, J., and PETIT, J. C., 1987, New evidence for the mechanisms of dissolution of silicate minerals, *in* STUMM, W., ed., Aquatic Surface Chemistry: New York, Wiley, p. 293–315.

SHEWMON, P. G., 1963, Diffusion in Solids: New York, McGraw-Hill, 203 p.

———, 1969, Transformations in Metals: New York, McGraw-Hill, 394 p.

SHIMIZU,N.; SEMET, M. P.; and ALLÉGRE, C. J., 1978, Geochemical applications of quantitative ion microprobe analysis: Geochim. Cosmochim. Acta, v. 42, p. 1321–1334.

SJÖBERG, L., 1989, Kinetics and non-stoichiometry of labradorite dissolution, *in* MILES, D. L., ed., Water-Rock Interaction: Rotterdam, Balkema, p. 639–642.

SPOSITO, G., 1984, The Surface Chemistry of Soils: New York, Oxford University Press, 234 p.

STEELE, I. M.; HERVIG, R. L.; HUTCHEON, I. D.; and SMITH, J.V., 1981, Ion microprobe techniques and analysis of olivine and low-Ca pyroxenes: Am. Mineral., v. 66, p. 526–546.

STUMM, W., and WOLLAST, R., 1990, Coordination chemistry of weathering: kinetics of the surface-controlled dissolution of oxide minerals: Rev. Geophysics, v. 28, p. 53–69.

THOMPSON, J. B., 1957, Local equilibrium in metasomatic processes, *in* ALBELSON, P. H., ed., Researches in Geochemistry, Vol. 1: New York, Wiley, p. 427–457.

TURNBULL, D., 1951, Atom Movements: Metals Park, Ohio, Am. Soc. Metals, 129 p.

WESTRICH, H. R.; CASEY, W. H.; and ARNOLD, G. W., 1989, Oxygen isotope exchange in the leached layer of labradorite feldspar: Geochim. Cosmochim. Acta, v. 53, p. 1681–1685.

WIELAND, E.; WEHRLI, B.; and STUMM, W., 1988, The coordination chemistry of weathering: III. A generalization on the dissolution rates of minerals: Geochim. Cosmochim. Acta, v. 52, p. 1969–1981.